AN UPPER BOUND ANALYSIS OF T-SHAPED EQUAL CHANNEL ANGULAR PRESSING

Kunxia Wei[1,2], Ping Liu[1] , Zhijun Ma[1], Wei Wei[1,2], Igor V. Alexandrov[3], Jing Hu[1,2]*
[1]School of Materials Science and Engineering, Changzhou University,Changzhou, P. R. China
[2]Jiangsu Key Laboratory of Materials Surface Science & Technology,Changzhou, P. R. China
[3]Department of Physics, Ufa State Aviation Technical University, Ufa, Russia

Received: 15.03.2015
Accepted: 26.03.2015

*Corresponding author: *e-mail: benjamin.wwei@163.com, Tel.:+86 519 8633 0095, School of Materials Science and Engineering, Changzhou University, Changzhou 213164, P. R. China*

Abstract
T-shaped equal channel angular pressing (T-shaped ECAP) is a novel process of severe plastic deformation (SPD). The maximum effective strain per pass in the T-shaped ECAP is larger than that in the ECAP. Deformation models of the T-shaped ECAP have been proposed by a designed grids deformation experiment considering the deformation dead zone (DDZ) formation or without it. Based on the deformation models, an upper bound approach has been used to analyse the T-shaped ECAP process. The effects of the plastic deformation zone (PDZ) angles and the friction factor on the relative pressing pressure and the DDZ are analysed. It is found that the relative pressing pressure increases with an increase of the angle β and the friction factor m, however, the DDZ decreases. The upper bound solution for the T-shaped ECAP with the DDZ is more close to the experimental load than that without the DDZ. The results show that there is a good agreement between the theoretical value and the measured maximum load required for the T-shaped ECAP conducting.

Keywords: T-shaped equal channel angular pressing, upper-bound analysis, grids deformation, severe plastic deformation

1 Introduction

Equal channel angular pressing (ECAP) is an effective route to refining coarse grains intoultrafine-grained or nanostructured states with the grain size of 0.1~1μm by means of large plastic shear deformation [1].The most advantage of ECAP is that the billet undergoes severe plastic deformation (SPD) with the maximum strain arriving at 1.15 after one single pass but the same cross-sectional geometry of the billet remains. Therefore, it is possible to repeat the pressings for a number of passes in order to achieve a high cumulative strain.

In order to optimize the ECAP process and obtain homogeneous nanostructured billets, many attempts have been made to analyse the ECAP process using deformation mechanics and finite element simulations [2-6]. Segal proposed three types of plastic deformation zone (PDZ) [2, 3]. The pressing pressure, the strain and the shear plane were investigated by the slip line theory. Due to the importance of the PDZ in optimization of the ECAP tool designs and processing variables, four different shapes, namely, i) the single shear plane, ii) the shearing fan, iii) the partial split PDZ mode, and IV) the full split PDZ mode, were assumed and compared to experimental results by Stoica *et al* [7]. Effects of the PDZ shape on the material flow during the ECAP were analysed by the FEM and the grid deformation patterns [8-13].

DOI 10.12776/ams.v21i1.539 p-ISSN 1335-1532
e-ISSN 1338-1156

Using the upper-bound analysis method, the PDZ shape can be predicted by optimizing the total power loss along all discontinuity and friction surfaces. Lee estimated the pressing pressure and the strain considering the single shear plane of the PDZ [14]. Taking into account the shearing fan with or without the deformation dead zone (DDZ), the upper-bound analysis was conducted [15-17]. Based on the rotational and linear velocity fields, the PDZ is divided into three rotational velocity fields, and then the force needed for ECAP was predicted [18]. Luis and Luri presented an upper-bound analysis of the required forces in the ECAP process considering a three dimensional geometry [19]. There is a good agreement between the upper-bound solution and experimental forces.

To obtain more severe mechanical working, T-shaped equal channel angular pressing (T-shaped ECAP) was developed by Rao et al [20,21]. Assuming that any part of the material will face a gradual change in its velocity in PDZ during the T-shaped ECAP, the strain and the extrusion pressure were calculated by the upper-bound analysis [22].Although the upper bound pressure showed a good agreement with the measured extrusion pressure, the proposed analytical deformation pattern was not verified by the experimental grids flow.

In the present work, rigid plastic deformation models incorporating the DDZ based on the grids deformation pattern have been proposed. The upper bound analysis of T-shaped ECAP has been carried out based on the developed models. The predicted pressing pressure from the upper bound analysis has been compared with the experimental loads.

2 Materials and methods

In the T-shaped ECAP process, the maximum effective strain ~1.39 per pass can be attained in comparison to 1.15 during the ECAP [22]. As shown in **Fig. 1**(a) during the T-shaped ECAP the billet is pressed down from the vertical channel to two laterally horizontal channels with the same inlet and the exit cross-sections. The biggest difference of the T-shaped ECAP in respect to the ECAP is that in the former case the velocity of the billet in the horizontal channel is half of that in the vertical channel, $v_1 = 2v_2 = v_0$. In the upper-bound method, it is assumed that there are a number of velocity discontinuity surfaces, on which the velocity suddenly changes [23].Consequently, the deformation model I without the DDZ is as shown in **Fig. 1**(a), in which it contains four rigid plastic bodies.

Talebanpour*et al*. proposed a continuous and gradual velocity field, in which the material flows along a specific streamline, which is the elliptical curve [22]. However, the deformation model was not examined by the experiments.

Pure Al (99.7 mass%) billets with a size of 12 × 12 × 80 mm^3 were annealed in vacuum at 673K for 1h. The yield stress, σ_0, has been 80 MPa. The shear yield stress, k, has been 46 MPa, where $k = \sigma_0/\sqrt{3}$. Two half-billets with size of 12×6×80 mm^3 have been cut, and one has been engraved with grids of 2×2 mm^2, another has been left free of grids. Then the two half-billets have been glued together and processed by the T-shaped ECAP. **Fig. 1**(b) shows the grids deformation pattern, in which it is evident to observe the DDZ formation at the bottom edge of the billet. Therefore, in order to describe this experimental observation it is reasonable to propose the deformation model presented in **Fig. 1**(c). The surfaces of the DDZ are simplified from the arc curves to straight lines because the DDZ is very small.

T-shaped ECAP has been conducted using a hydraulic press of 100 T capacity at room temperature. The billets were pressed one pass using a molybdenum disulfide lubricant. The pressing speed is 1 mm s^{-1}. The load-displacement curve has been recorded during the T-shaped ECAP to compare with the upper bound solutions.

DOI 10.12776/ams.v21i1.539 p-ISSN 1335-1532
e-ISSN 1338-1156

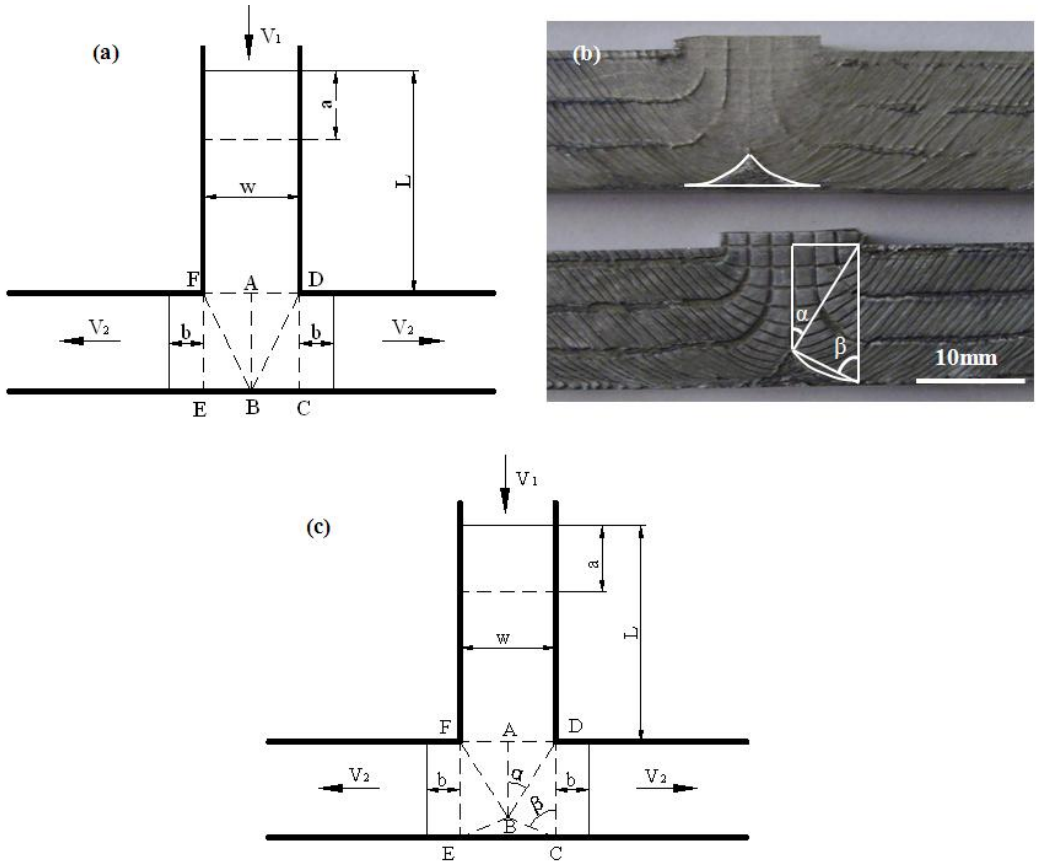

Fig. 1 Deformation models: (a) the model I without the DDZ, (b) the experimental grids deformation, and (c) the model II with the DDZ

3 Upper bound analysis of T-shaped ECAP

On the basis of an extremum principle, the upper-bound solution is equal to or higher than the actually required force in metal forming process. The upper bound on power is defined as:

$$J^* \leq 2k \int_V \overline{\frac{1}{2}\varepsilon_{ij}\varepsilon_{ij}}dV + \int_{S_\Gamma} k\,\Delta v\,ds + \int_{S_f} mk\,\Delta v_f\,ds - \int_{S_i} T_i v_i ds \quad (1.)$$

where J^* is the actual power that must be supplied to perform the plastic deformation. k is the shear yield stress, ε_{ij} is the strain rate tensor, V is the volume of the deformationzone, S_Γ and S_f are the area of velocity discontinuity and frictional surfaces, correspondingly, $|\Delta v|$ and $|\Delta v_f|$are the relativevelocity on S_Γ and S_f, correspondingly, mis the friction factor, S_i is the area where the tractions may occur,$T_i$is the externaltraction force, $v_i$isthe velocity of the surfacesunder the force T_i.

The first term in right side of Eq. (1) is the internal power consumed in the PDZ. It is assumed that the PDZ is rigid. So, the first term can be neglected. In the T-shaped ECAP process there is no external tension. So, the last term is equal to zero.

DOI 10.12776/ams.v21i1.539 p-ISSN 1335-1532
e-ISSN 1338-1156

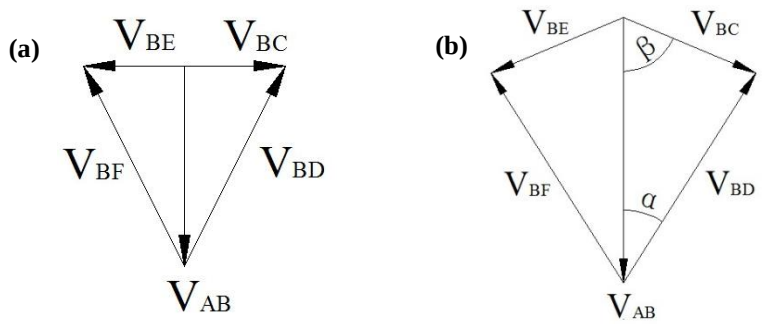

Fig. 2 The velocity hodograph: (a) the model I without the DDZ, and (b) the model II with the DDZ

3.1 The deformation model I (without the DDZ)

In **Fig. 1**(a), BDand BFare velocity discontinuity planes. The velocity hodograph is as shown in **Fig. 2**(a).v_{BD} and v_{BF} are the relative velocities along the plane BDand BF, correspondingly. v_{BC} and v_{BE} are the relative velocities of the material against the die walls, correspondingly. The power for the deformation of material of w in width,W, is given by

$$\mathbf{W = W_i + W_{S_{BDF}} + W_{S_{BCD}} + W_{S_{BEF}} + W_{S_{walls}}} \tag{2.}$$

Here, W_i is the power dissipated on the velocity discontinuity planes.

$$\mathbf{W_i = k\ S_{BC} \cdot v_{BC} + S_{BD} \cdot v_{BD} + S_{BF} \cdot v_{BF} + S_{BE} \cdot v_{BE}\ = 3kw^2 v_0} \tag{3.}$$

$W_{S_{BDF}}$, $W_{S_{BCD}}$ and $W_{S_{BEF}}$ are the power dissipated on the friction between the PDZ and the die front and back walls, correspondingly.

$$\mathbf{W_{S_{BDF}} = mkS_{BDF} \cdot v_{AB} = mkw^2 v_0} \tag{4.}$$

$$\mathbf{W_{S_{BCD}} = mkS_{BCD} \cdot v_{BC} = \frac{1}{4} mkw^2 v_0} \tag{5.}$$

$$\mathbf{W_{S_{BEF}} = mk(S_{BE} \cdot v_{BE} + S_{BEF} \cdot v_{BE}) = \frac{1}{4} mkw^2 v_0} \tag{6.}$$

$$\mathbf{W_{S_{walls}} = mkv_1 \cdot 4w(L - a) + mkv_2 \cdot\ 8wb\ = 4mkw(L - a + b)v_0} \tag{7.}$$

where a is the stroke of the punch, b is the length of the material which passes the channel intersection region. $b = \frac{1}{2}a$ due to the volume constancy. When the friction outside of the PDZ is neglected, substituting Eq. (3)-(6) into Eq. (2), the power W can be expressed as

$$\mathbf{W = (3 + 1.5m)kw^2 v_0} \tag{8.}$$

The external power, J, is given by $J = qw^2 v_0$, where q is the average pressing force per unit area. Therefore the following relation is obtained.

DOI 10.12776/ams.v21i1.539 p-ISSN 1335-1532
e-ISSN 1338-1156

$$q \le (3 + 1.5m)k \tag{9.}$$

3.2 The deformation model II (with the DDZ)

In **Fig. 1**(c), BD, BF,BC and BEare velocity discontinuity planes. The velocity hodograph is as shown in **Fig. 2**(b).ν_{BD}, ν_{BF}, ν_{BC} and ν_{BE} are the relative velocities along the plane BD, BF,BC and BE, correspondingly. The power for the deformation of material of w in width, W, is given by

$$\mathbf{W = W_i + W_{S_{BDF}} + W_{S_{BCD}} + W_{S_{BEF}} + W_{S_{walls}}} \tag{10.}$$

Here, W_i is the power dissipated on the velocity discontinuity planes.

$$\mathbf{W_i = k\ S_{BC} \cdot \nu_{BC} + S_{BD} \cdot \nu_{BD} + S_{BF} \cdot \nu_{BF} + S_{BE} \cdot \nu_{BE}}$$

$$= \mathbf{2k}\ \frac{w^2}{2\sin\beta} \cdot \frac{\nu_0 \sin\alpha}{\sin(\pi-\alpha-\beta)} + \frac{w^2}{2\sin\alpha} \cdot \frac{\nu_0 \sin\beta}{\sin(\pi-\alpha-\beta)} = \frac{kw^2\nu_0}{\sin(\alpha+\beta)} \cdot \frac{\sin\alpha}{\sin\beta} + \frac{\sin\beta}{\sin\alpha} \tag{11.}$$

$W_{S_{BDF}}$, $W_{S_{BCD}}$ and $W_{S_{BEF}}$ are the powers dissipated on the friction between the PDZ and the die front and back walls, correspondingly.

$$\mathbf{W_{S_{BDF}} = mkS_{BDF} \cdot \nu_{AB} = 2mk}\ \frac{1}{2}\mathbf{w} \cdot \frac{w}{2\tan\alpha}\ \mathbf{\nu_0} = \frac{mkw^2\nu_0}{2\tan\alpha} \tag{12.}$$

$$\mathbf{W_{S_{BCD}} = mkS_{BCD} \cdot \nu_{BC} = 2mk}\ \frac{1}{2} \cdot \frac{w}{2\sin\beta} \cdot \mathbf{w}\sin\boldsymbol{\beta}\ \cdot \frac{\nu_0 \sin\alpha}{\sin(\pi-\alpha-\beta)} = \frac{mkw^2\nu_0 \sin\alpha}{2\sin(\alpha+\beta)} \tag{13.}$$

$$\mathbf{W_{S_{BEF}} = mkS_{BEF} \cdot \nu_{BE}} = \frac{mkw^2\nu_0 \sin\alpha}{2\sin(\alpha+\beta)} \tag{14.}$$

When the friction outside of the PDZ is neglected, $W_{S_{walls}}$ is equal to zero. Substituting Eq. (11) ~ (14) into Eq. (10), the powerW can be expressed as

$$\mathbf{W} = \frac{kw^2\nu_0}{\sin(\alpha+\beta)} \cdot \frac{\sin\alpha}{\sin\beta} + \frac{\sin\beta}{\sin\alpha}\ + \mathbf{mkw^2\nu_0}\left(\frac{1}{2\tan\alpha} + \frac{\sin\alpha}{\sin(\alpha+\beta)}\right) \tag{15.}$$

The external power, **J**, is given by $\mathbf{J = qw^2\nu_0}$, where **q** is the average pressing force per unit area. Therefore the following relation is obtained.

$$\mathbf{q} \le \frac{k}{\sin(\alpha+\beta)} \cdot \frac{\sin\alpha}{\sin\beta} + \frac{\sin\beta}{\sin\alpha}\ + \mathbf{mk}\left(\frac{1}{2\tan\alpha} + \frac{\sin\alpha}{\sin(\alpha+\beta)}\right) \tag{16.}$$

When $\beta = 90^{\circ}$and $\alpha = 26.565^{\circ}$, the DDZ disappears. Thus the deformation model II is identical to the model I, and then the Eq. (16) is reduced to the Eq. (9).

4 Results and discussion

From **Fig.1** (c) and Eq. (16), it follows that the development of the DDZ and the pressing force are affected by the anglesα, β and the friction factor m. Taking the midpoint of the segment CD as the circle center and the half of the segment CD as the radius, the line EC and the circle are

DOI 10.12776/ams.v21i1.539 p-ISSN 1335-1532
e-ISSN 1338-1156

tangent to the point C, and the line AB tangent to the point B. At this moment, the largest DDZ comes into being, and $\alpha = \beta = 45^{\circ}$ as shown in **Fig. 3**(a). However, it is not easy for the billet itself to develop the largest DDZ.

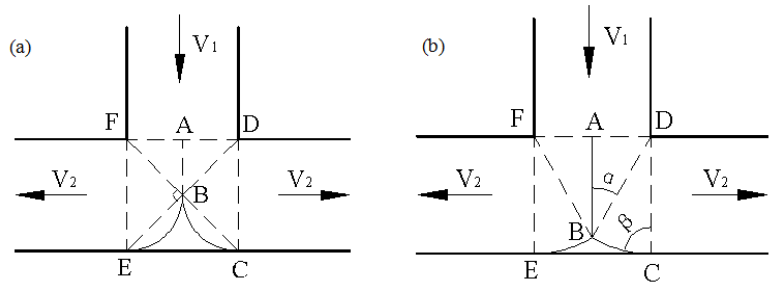

Fig. 3 Effect of the angle β on the DDZ (a) $\beta = 45^{\circ}$and (b) $\beta = 75$

When BD= CD, namely, the pointB and C are on the same circle taking the point D as the center, the line EC and the line AB, tangent to the circle at the point C, intersect at the point B, respectively. In a similar way, the length EF= BF taking the point F as the center of a circle. In this case, a billet could flow in a gradual and continuous way from the vertical channel to the horizontal channels, and $\alpha = 30^{\circ}$and$\beta = 75^{\circ}$ as shown in **Fig. 3**(b). Thus, the angle β is ranged from $45^{\circ}$to 90°.

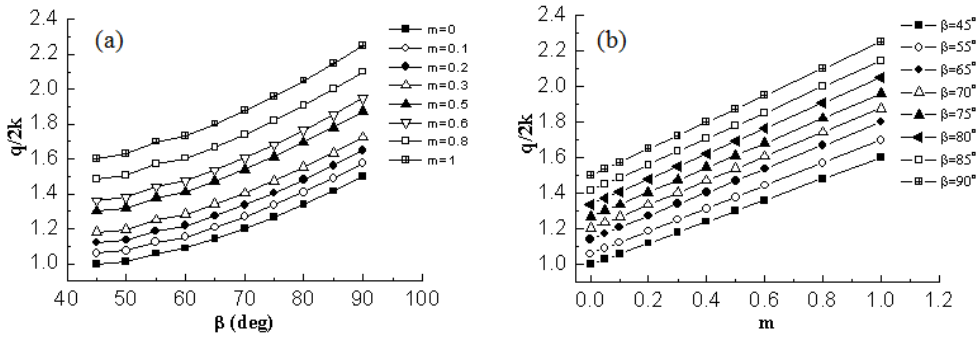

Fig. 4 Effect of (a) the angle β and (b) the constant friction factor m on the relative pressurecalculated by Eq. (16)

Fig. 4 shows the effect of the angle β and the friction factor m on the relative pressure. In **Fig. 4**(a), the relative pressure increases with an increase of the angle β, correspondingly, the DDZ decreases. For the ideally plastic material, the friction coefficient m varies between0 and 1. The constant friction factor m has a significant effect on the relative pressure as shown in **Fig. 4**(b). The friction force along all of the surfaces between the material and the die is modelled by mk. For commercial pure aluminum, the constant friction factor m is assumed as 0.1 [18, 24]. Taking into account the existence of the friction force along all of the surfaces between the material and the die, the upper-bound solution to the T-shaped ECAP has been compared to the experimental load-displacement curve for the first pass in **Fig. 5**. Without consideration of the DDZ, the upper bound pressure predicted by Eq. (9) is 36.4 KN, 28% higher than the maximum experimental

DOI 10.12776/ams.v21i1.539 p-ISSN 1335-1532
e-ISSN 1338-1156

load for the T-shaped ECAP. In case of $\beta = 75^{\circ}$ with the DDZ, the upper bound pressure predicted by Eq. (16) is 33.1 KN, 16% higher than the maximum experimental load. In fact, β is close to 65° from the grids deformation pattern in **Fig. 1**(b). The predicted pressure is 31.3 KN, which is very close to the maximum experimental load 28.5 KN, the difference between them is only 10%, showing a good agreement between the theoretical model and experiments.

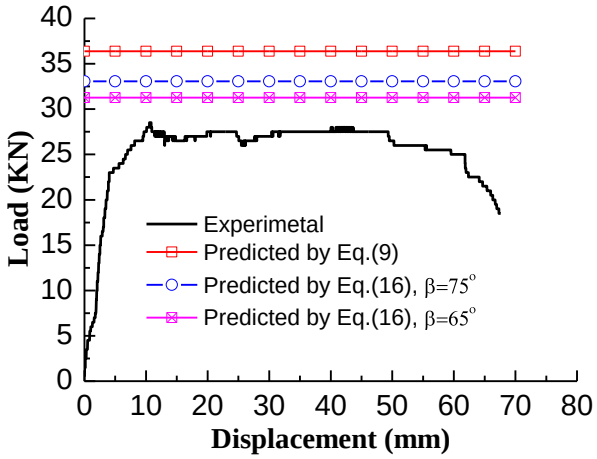

Fig. 5 A typical load-displacement curve for the first pass in the T-shaped ECAP process in comparison to the upper bound solutions

Furthermore, the angle β measured from the grids deformation in **Fig. 1**(b) is 65°, less than the theoretical value 75°. The DDZ decreases with an increase of the angle β in **Fig. 3**. It indicates that the DDZ increases with increasing the friction factor. It is well in agreement with that in the ECAP process, in which the PDZ becomes larger with the friction factor due to the DDZ increase [12, 15, 18, 25].

5 Conclusions

An upper bound approach has been used to analyse the T-shaped ECAP process based on the proposed deformation models. The effects of the PDZ angles and the friction factor on the relative pressing pressure and the DDZ have been analysed. The following conclusions can be outlined:

1. Deformation models taking into account the existence or absence of deformation dead zone (DDZ) in the T-shaped ECAP process are proposed based on the results of a designed grids deformation experiment.
2. The DDZ and the pressing force in the T-shaped ECAP are affected by the anglesα, β and the friction factor m.
3. The relative pressing pressure increases with an increase of the angle β and the friction factorm, however, the DDZ decreases.
4. The upper bound solution to the T-shaped ECAP with DDZ is more close to the experimental load than that without DDZ. From the grids deformation pattern it follows that the angle β is close to 65°. In such a case, the difference between the predicted pressure and the maximum experimental load is only 10%, showing a good agreement

DOI 10.12776/ams.v21i1.539 p-ISSN 1335-1532
e-ISSN 1338-1156

between the theoretical value and the measured maximum load required for T-shaped ECAP.

References

[1] C. J. Luis, I. Puertas, R. Luri, J. León, D. Salcedo, I. Pérez: Materials and Manufacturing Processes, Vol. 27,2012, No. 12, p. 1276-1284, DOI:10.1080/10426914.2012.663128
[2] V. M. Segal: Materials Science and Engineering A, Vol. 271, 1999, No. 1-2, p. 322-333, DOI:10.1016/S0921-5093(99)00248-8
[3] V. M. Segal: Materials Science and Engineering A, Vol. 345, 2003, No. 1-2, p. 36-46, DOI: 10.1016/S0921-5093(02)00258-7
[4] A. V. Perig, I. G. Zhbankov, V. A. Palamarchuk: Materials and Manufacturing Processes, Vol. 28, 2013, No. 8, p. 910-915, DOI: 10.1080/10426914.2013.792420
[5] A. V. Perig, I. G. Zhbankov, I. A. Matveyev, V. A. Palamarchuk: Materials and Manufacturing Processes, Vol. 28, 2013, No. 8, p. 916-922, DOI: 10.1080/10426914.2013.792417
[6] A. V. Perig, A. F. Tarasov, I. G. Zhbankov, S. N. Romanko: Materials and Manufacturing Processes, Vol. 30, 2015, No. 2, p. 222-231, DOI: 10.1080/10426914.2013.832299
[7] G. M. Stoica et al.: Materials Science and Engineering A, Vol. 410-411, 2005, p. 239-242, DOI: 10.1016/j.msea.2005.08.186
[8] F. R. F. Silva, N. Mederiros, L. P. Moreira, J. F. C. Lins, J. P. Gouvêa: Materials Science and Engineering A, Vol. 546, 2012, p.180-188, DOI: 10.1016/j.msea.2012.03.049
[9] G. Deng et al.: Computational Materials Science, Vol. 81, 2014, p. 79-88, DOI: 10.1016/j.commatsci.2013.07.006
[10] I. J. Beyerlein, C. N. Tomé: Materials Science and Engineering A, Vol. 380, 2004, No. 1-2, p. 171-190, DOI: 10.1016/j.msea.2004.03.063
[11] S. Li, M. A. M. Bourke, I. J. Beyerlein, D. J. Alexander, B. Clausen: Materials Science and Engineering A, Vol.382, 2004, No. 1-2, p. 217-236, DOI: 10.1016/j.msea.2004.04.067
[12] T. Kvačkaj, R. Kočiško, A. Kováčová: Chemicke Listy, Vol. 106, 2012,No. s3, p.464-467
[13] T. Kvačkaj, et al.: Kovove Materialy, Vol. 45, 2007, No. 5,p. 249-254
[14] D. N. Lee: Scripta Materialia, Vol. 43,2000, No. 2, p. 115-118, DOI: 10.1016/S1359-6462(00)00377-8
[15] B. S. Altan, G. Purcek, I. Miskioglu: Journal of Materials Proccessing Technology,Vol. 168, 2005, No. 1, p. 137-146, DOI: 10.1016/j.jmatprotec.2004.11.010
[16] M. H. Paydar, M. Reihanian, R. Ebrahimi, T. A. Dean, M. M. Moshksar: Journal of Materials Proccessing Technology, Vol. 198,2008, No. 1-3, p. 48-53, DOI: 10.1016/j.jmatprotec.2007.06.051
[17] A. R. Eivani, A. K. Taheri: Journal of Materials Proccessing Technology, Vol. 182,2007, No. 1-3, p. 555-563, DOI: 10.1016/j.jmatprotec.2006.09.021
[18] M. Reihanian, R. Ebrahimi, M. M. Moshksar: Materials &Design, Vol. 30, 2009, No. 1, p. 28-34, DOI: 10.1016/j.matdes.2008.04.059
[19] C. J. Luis Pérez, R. Luri: Mechanics of Materials, Vol. 40,2008, No. 8, p. 617-628, DOI: 10.1016/j.mechmat.2008.02.003
[20] V. Srinivas Rao, B. P. Kashyap, N. Prabhu, P. D. Hodgson: Materials Science and Engineering A, Vol. 486, 2008, No. 1-2,p. 341-349, DOI: 10.1016/j.msea.2007.09.004
[21] B. Talebanpour, R. Ebrahimi, K. Janghorban: Materials Science and Engineering A, Vol. 527, 2009, No. 1-2, p. 141-145, DOI: 10.1016/j.msea.2009.07.040

[22] B. Talebanpour, R. Ebrahimi: Materials &Design, Vol. 30,2009, No. 5, p. 1484-1489, DOI: 10.1016/j.matdes.2008.08.006
[23] B. Avitzur, W. Pachla: Journal of Engineering & Industry, Vol. 168, 1986, p. 295-306
[24] J. Jung, S. C. Yoon, H. J. Jun, H. S. Kim: Journal of Materials Engineering and Performance, Vol. 22, 2013, No. 11, p. 3222-3227, DOI: 10.1007/s11665-013-0632-x
[25] T. Kvačkaj, J. Bidulská, R. Kočiško, R. Bidulský: Effect of Severe Plastic Deformation on the Properties and Structural Developments of High Purity Al and Al-Cu-Mg-Zr Aluminium Alloy. In.: *Aluminium Alloys, Theory and Applications*,edited by T. Kvackaj, R. Bidulský, InTech, Rijeka, 2011, p. 3-26, DOI: 10.5772/14425

Acknowledgements

Authors are grateful for the support of experimental works by the Natural Science Foundation of Jiangsu Province, P. R. China under grant BK2012594 and BK20131144, the Science Project of Changzhou, P. R. China under grant No. CZ20130021, the Project Funded by the Priority Academic Program Development of Jiangsu Higher Education Institutions and The Ministry of Education and Science of the Russian Federation within the Framework of the Design Part of the State Task No.11.2540.2014/K Educational Organization of Higher Education.